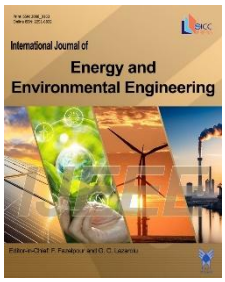

Int. J. Energy Environ. Eng., 2026; 17(1): 65-73

International Journal
of
Energy and Environmental Engineering (IJEEE)

https://doi.org/10.57647/ijeee.2026.1701.05

Research Article

Quantification of Microplastics and Total Petroleum Hydrocarbons in Seawater and Sediments of the Southwestern Caspian Sea

Roghayeh Shahbazi[1], Ebrahim Fataei[1*], Ali Mehdinia[2], Maryam Hazrati Niari[3*], Hossein Saadati[1]

[1]*Department of Environmental Science and Engineering, Ard.C., Islamic Azad University, Ardabil, Iran*
[2]*Iranian National Institute for Oceanography and Atmospheric Science, Tehran, 1411813389, Iran*
[3]*Lung Diseases Research Center, Ardabil University of Medical Sciences, Ardabil, Iran*

***Corresponding author:** eb.fataei@iau.ac.ir, m.hazrati@arums.ac.ir, m.hazratii@yahoo.com

Article History:

Received:
14 November 2025

Revised:
25 January 2026

Accepted:
12 February 2026

Published in Issue:
31 March 2026

Abstract

Coastal environments are increasingly threatened by emerging contaminants; however, integrated assessments of multiple pollutant classes remain scarce. This study provides a simultaneous investigation of microplastics (MPs) and total petroleum hydrocarbons (TPHs) in seawater and sediments along the southwestern coast of the Caspian Sea. Samples were collected from fourteen coastal stations during the dry season. MPs were characterized by type, size, shape, color, and polymer composition using microscopy and Raman spectroscopy, while TPHs were quantified using GC-MS. The results revealed MP abundances ranging from 0.05 to 2.35 particles L^{-1} in water and from 2.01 to 24.13 particles kg^{-1} in sediment. Fibers and fragments in the 100–500 µm size class were dominant, with polyethylene (PE) and polyethylene terephthalate (PET) identified as the most prevalent polymers. TPH concentrations varied from not detected to 20.152 µg L^{-1} in water and from 8.37 to 1835.29 µg kg^{-1} in sediment. Spatial analysis showed no overlap between the contamination hotspots of MPs and TPHs, indicating distinct sources and transport pathways. This concurrent assessment underscores a complex contamination profile in the region and highlights potential ecological risks from both physical and chemical stressors. The distinct spatial patterns provide critical information for designing targeted pollution control measures.

Keywords: Microplastics; Petroleum pollution; Sediments pollutant; Water pollutants, Caspian sea

Cite this article: Shahbazi R., Fataei E., Mehdinia A., Hazrati Niari M., & Saadati H., Quantification of Microplastics and Total Petroleum Hydrocarbons in Seawater and Sediments of the Southwestern Caspian Sea. Int. J. Energy Environ. Eng., 2026; 17(1): 65-73.
https://doi.org/10.57647/ijeee.2026.1701.05

1. Introduction

Coastal marine environments are increasingly exposed to complex mixtures of emerging contaminants, among which microplastics (MPs) and petroleum-derived pollutants have received considerable scientific and regulatory attention. MPs (plastic particles smaller than 5 mm) are now recognized as persistent contaminants that accumulate in surface waters, water columns, sediments, and marine food webs [1-3]. Numerous

studies have documented their widespread occurrence and the associated ecological risks across marine ecosystems worldwide [4-6] Because of their persistence and mobility, MPs can be transported over long distances and deposited in sediments, where they may be ingested by organisms or cause physical harm such as gastrointestinal blockage and impaired feeding [7-9]. Beyond their physical impacts, MPs can act as vectors for chemical contaminants by adsorbing hydrophobic compounds, including petroleum hydrocarbons, thus potentially facilitating long-range transport and altering contaminant bioavailability [10-12]. Total petroleum hydrocarbons (TPHs) are another major class of persistent and potentially toxic contaminants in coastal environments, originating from oil extraction, urban runoff, maritime traffic, and industrial discharges. Elevated TPH concentrations have been associated with mutagenic, carcinogenic, and sublethal effects in aquatic organisms, which underscores the need for robust environmental monitoring [13, 14]. In the Caspian Sea—the world's largest enclosed inland water body—concern about marine pollution has intensified recently. Several studies have reported MPs in different environmental matrices along the southern and southwestern coasts. For example, Nematollahi et al. (2020) reported the occurrence and characteristics of MPs in coastal waters and sediments of the southern Caspian Sea. Manbohi et al. (2021) documented spatial variability in MP abundance between inshore and offshore waters, highlighting the roles of hydrodynamics and land-based activities. More recent studies have reported the accumulation of MPs in sediments, riverine inputs, and zooplankton, indicating their entry into coastal food webs [15, 16]. Although petroleum hydrocarbons have been detected in sediments and coastal waters of the Caspian Sea, regional assessments have typically focused on either TPH concentrations or specific polycyclic aromatic hydrocarbons (PAHs), rather than on joint evaluations with MPs. Regional surveys such as Emadi Jamali et al. (2020) have reported elevated TPH levels in southern Caspian sediments and attributed these levels to urban effluents, oil-related activities, and riverine discharges [13]. Despite these efforts, integrated and simultaneous assessments of MPs and TPHs in the same environmental matrices remain scarce in the Caspian Sea region. This gap is critical because the co-occurrence of MPs and petroleum hydrocarbons could modify contaminant transport pathways, exposure scenarios, and ecological risks. Moreover, the semi-enclosed nature of the Caspian Sea may enhance retention and accumulation of both pollutant classes, reinforcing the need for comprehensive and spatially resolved investigations. Therefore, this study provides the first concurrent investigation of MPs and TPHs in seawater and sediments from the southwestern Caspian Sea. By characterizing MP abundance, size distribution, morphology, color, and polymer composition alongside quantitative TPH measurements, we aim to clarify the region's contamination profile and provide baseline data for future studies on pollution sources and environmental impacts.

2. Materials and methods

2.1. Study area

The Caspian Sea is the world's largest enclosed inland water body, covering nearly 436,000 km², with a length of 1200 km, an average width of 330 km, and a mean depth of 180 m. It is bordered by Iran, Azerbaijan, Russia, Kazakhstan, and Turkmenistan. Along the southern basin, where the Iranian coast lies, salinity ranges between 12–13 ppt with slightly alkaline sodium–chloride water. The Iranian coastline spans about 820 km across Gilan, Mazandaran, and Golestan provinces, receiving freshwater and sediments from over 60 rivers and streams. The Sefidrud River is the largest contributor of water and contaminants. The southern Caspian has a humid subtropical climate, and human activities—including agriculture, fisheries, tourism, and industry—have increased environmental pressures in recent decades [5, 17]. This study focused on the western Iranian coast, between Astara and Bandar Anzali (approx. 118 km), a dynamic system of sandy beaches, river mouths, and the Anzali Lagoon. The west–east coastal current plays a key role in dispersing contaminants. The precise geographical coordinates (latitude and longitude) of each sampling location are listed in Table 1. The study area and the locations of the MPs sampling sites are shown in Fig. 1. Seawater and surface sediment samples were collected simultaneously from multiple stations to assess contaminant levels and spatial distribution.

2.2. Sampling and Sample Preparation

Sampling was carried out during the dry season in June 2025. Fourteen stations were selected for both water and sediment sampling. Water was collected linearly along the shoreline at a depth of approximately 20 cm using a 12-V DC pump. At each station, five 1-L water subsamples were collected and combined to form a 5-L composite sample. This process was repeated to obtain a second 5-L composite, and the two composites were then combined to create a single 10-L sample per station. The 10-L samples were passed through a 25-µm stainless-steel sieve, and particles retained on the sieve were rinsed into 100 mL glass bottles with deionized water. After thorough mixing, aliquots were taken from each composite sample for further analysis [18, 19]. Sediment samples were collected along the shoreline. At each station, a 1 × 1 m metal frame was placed on the sediment surface and pressed down approximately 5 cm. Sediment inside the frame (~3 kg) was scooped and transported to the laboratory. All samples were handled using pre-cleaned glassware to avoid contamination, and blank controls were processed alongside field samples.

2.3. Samples Extraction

2.3.1. *Water Samples*

Water samples were treated with 10 mL of 30% hydrogen peroxide (H_2O_2, Merck, Germany) at room temperature for 48 h to digest organic matter [20-22]. Samples were then filtered through 1.2-µm glass microfiber filters, oven-dried at 60 °C, and stored in Petri

10.57647/ijeee.2026.1701.05

dishes in a desiccator until further microscopic and spectroscopic analysis [23].

2.3.2. *Sediment Samples*

Sediment samples were dried at 60 °C to constant weight, sieved through a 4.75-mm stainless-steel mesh, and 1 kg of dried sediment from each station was used for analysis. MPs were isolated using a two-step density separation procedure based on air-induced overflow (AIO).

1. Step 1 – NaCl flotation: Sediments were fluidized in a saturated NaCl solution (density 1.2 g/cm³) to separate MPs from the bulk sediment. Small particles were collected through a 25-µm stainless-steel sieve and rinsed with distilled water.
2. Step 2 – NaI flotation: The remaining sediment was treated with 60% (w/w) NaI solution (density 1.8 g/cm³). Low-density MPs floated to the surface and were collected by vacuum filtration using 0.45-µm nitrocellulose filters. Filters were rinsed to remove salts and dried for further analysis.

Organic matter remaining on the filters was digested with H_2O_2 (30 mL, 72 h at room temperature), and an additional filtration step was performed to remove residual NaI [24-26].

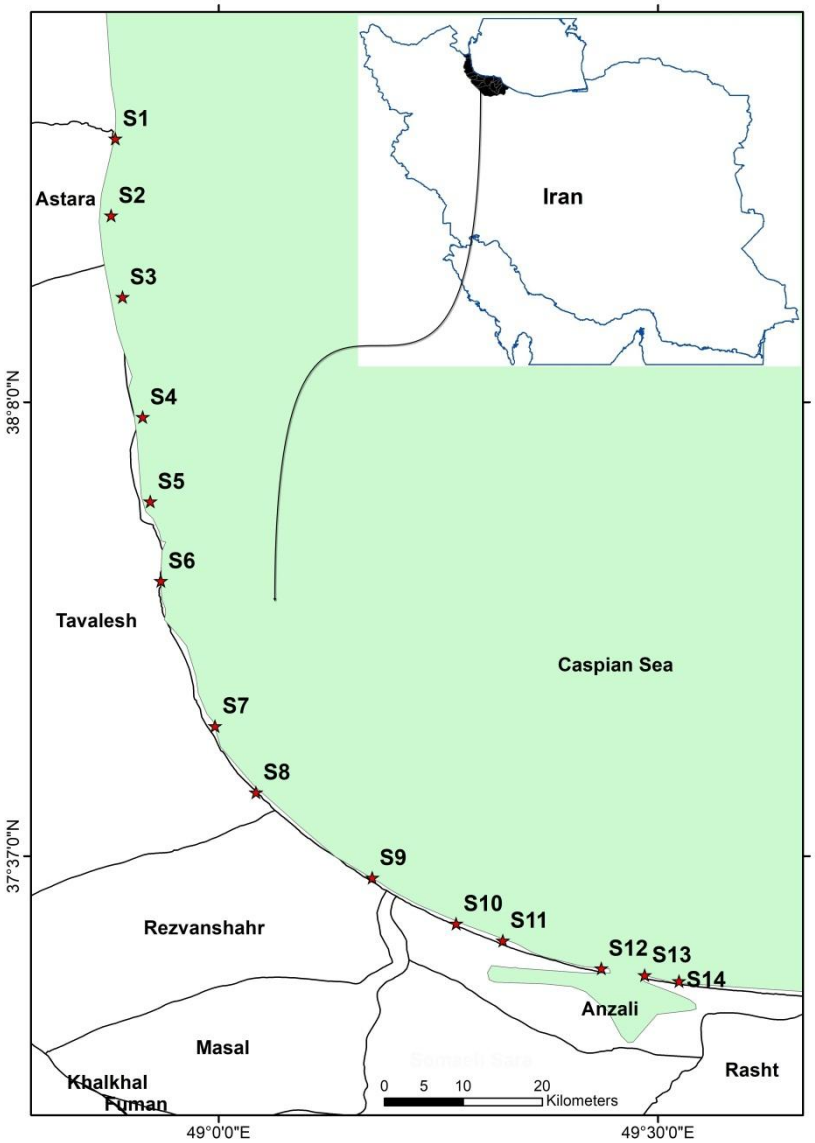

Figure 1. Study area and locations of microplastic sampling sites

Table 1. Geographic coordinates of sampling stations

Station Code	Location Name	Latitude (DMS)	Longitude (DMS)	Latitude (decimal °N)	Longitude (decimal °E)	Sample Type
S1	Astara	38°25'44.76"N	48°52'19.20"E	38.429100	48.872000	Sediment and Water
S2	Lavandevil	38°18'32"N	48°52'13"E	38.308889	48.870278	Sediment and Water
S3	Chubar	38°10'44"N	48°53'34"E	38.178889	48.892778	Sediment and Water
S4	Haviq	38°09'35.22"N	48°52'38.55"E	38.159782	48.877376	Sediment and Water
S5	Khotbeh Sara	38°01'51"N	48°54'39"E	38.030833	48.910833	Sediment and Water
S6	Lisar	37°57'24.74"N	48°54'25.61"E	37.956872	48.907113	Sediment and Water
S7	Hashtpar (Talesh)	37°48′00″N	48°54′00″E	37.8000°	48.9000°	Sediment and Water
S8	Khaleh Sara	37°24'41"N	49°05'35"E	37.411390	49.093060	Sediment and Water
S9	Rezvanshahr	37°32'57.80"N	49°08'08.88"E	37.549389	49.135799	Sediment and Water
S10	Tazehabad	37°28'26"N	49°29'07"E	37.473889	49.485278	Sediment and Water
S11	Kapurchal	37°32'55.68"N	49°14'03.12"E	37.548800	49.234200	Sediment and Water
S12	Kuchak Mahalleh	37°32'14.10"N	49°15'42.60"E	37.537250	49.261830	Sediment and Water
S13	Sangachin	37°31'02"N	49°18'35"E	37.517220	49.309720	Sediment and Water
S14	Bandar Anzali	37°28'23.5"N	49°27'28.4"E	37.473200	49.457900	Sediment and Water

2.4. MP particles identification

MP particles on each filter were identified using a binocular optical microscope (Carl-Zeiss, Weet, Germany) with magnification up to ×120 (Fig. 2). Particle size measurements were performed using the microscope's built-in imaging software, and the measurements were therefore conducted in a semi-manual, digitally assisted manner. Particle size was classified into seven categories based on length (L): 100–500 µm, 500–1000 µm, 1000–1500 µm, 1500–2000 µm, 2000–2500 µm, 2500–3000 µm, and >3000 µm. Particles smaller than 100 µm were not considered due to the identification limits of the microscope used. MP particles were classified by shape into three types: fiber, film, and fragment. The color of the particles was also recorded and analyzed. Of the 350 particles visually identified as potential MPs, a representative subset of 85 particles (approximately 25%) covering all morphologies and size classes were analyzed by Raman spectroscopy for polymer identification. The extracted MPs were mounted on copper adhesive tape for subsequent analysis and characterization. Raman spectroscopy was used to identify the polymer types, employing a Teksan Raman785-G100 instrument equipped with a 785 nm laser. Depending on the particle size, either 40× or 60× objective lenses were selected to enhance focus and improve spectral resolution. The laser power was adjusted between 10% and 100% according to the sensitivity of each particle to minimize thermal effects or potential structural alteration. Exposure times ranged from 3 to 30 minutes to ensure well-defined and

high-quality Raman spectra. Spectra were collected over a range of approximately 400–3200 cm^{-1}, which is suitable for detecting diagnostic vibrational modes of the most common polymers found in MPs. Polymer identification was based on characteristic Raman bands, including: C–H stretching vibrations in the 2800–3000 cm^{-1} region, typical of many organic polymers such as PE, PP, PS, and PVC. Peaks near ~2850 and ~2880 cm^{-1} are associated with PE, whereas peaks around 2920–2960 cm^{-1} are characteristic of PP and PS. Aromatic C=C stretching between 1580–1620 cm^{-1}, useful for identifying aromatic polymers such as PS and PET. C–H bending (scissoring) in the 1350–1470 cm^{-1} region, including a peak around 1440 cm^{-1} for PE and ~1375 cm^{-1} for PP. C–C skeletal stretching at 1050–1150 cm^{-1}, corresponding to polyolefin backbone vibrations, with a well-known peak at ~1128 cm^{-1} for PE. C–O and C=O stretching modes in the 1000–1300 cm^{-1} and 1670–1750 cm^{-1} ranges, respectively, indicative of oxygen-containing polymers such as PET, PMMA, and PC. C–Cl stretching vibrations around 600–700 cm^{-1}, including a distinctive peak near ~638 cm^{-1} associated with PVC. Additional aromatic ring modes, including peaks at ~620–650 cm^{-1}, ~1000 cm^{-1}, 1025–1040 cm^{-1}, and 1200–1260 cm^{-1}, commonly observed in PS and PET. After collecting the Raman spectra, the data were processed in Origin software to reduce noise, remove background peaks, and perform baseline correction. In the final step, the extracted characteristic peaks were compared with reference spectra available in established databases. Polymer types for each sample were identified based on the positions and intensities of these peaks.

2.5. Extraction and Analysis of TPH

TPH in both sediment and water samples were extracted using an optimized liquid–solid and liquid–liquid extraction method [27]. Sediment samples were first dried using a freeze-dryer for 72 hours and sieved through a 250 µm mesh. For extraction, 5 g of sediment or 1 L of water was spiked with 1280 ppb p-Terphenyl-d14 as a surrogate standard. Sediments were sonicated with 20 mL of a 50:50 dichloromethane–acetone mixture, centrifuged, and the supernatant collected. Water samples were extracted sequentially with dichloromethane and n-hexane using a separatory funnel. Extraction steps for both matrices were repeated to ensure complete recovery. Extracts were concentrated using a rotary evaporator, exchanged to n-hexane, cleaned up through a silica gel–alumina column, and finally reduced to a volume of 200–500 µL under nitrogen. One microliter of the resulting extract was injected into a GC-MS system (Agilent 6890N) for TPH quantification.

Figure 2. Representative optical micrographs of the collected microplastic

2.6. Quality Control and Quality Assurance

All samples were analyzed by the same trained analyst to ensure consistency. Laboratory glassware was carefully cleaned with phosphate-free soap, rinsed twice with distilled water, soaked in 10% HNO_3 for 24 h, rinsed twice again with double-distilled water, and left semi-closed to dry at room temperature. Laboratory benches were thoroughly cleaned with ethanol prior to analysis. All reagents and solutions were filtered through 2 µm S&S blue band filters. Plastic laboratory equipment and synthetic garments were avoided, and cotton gloves and laboratory coats were used throughout. To monitor potential contamination of airborne MPs, blank control samples were kept open on the laboratory bench during experiments; no contamination was detected. For TPH analysis, procedural blanks and surrogate standards were included to ensure the accuracy and reliability of extraction and quantification. Instrument precision and accuracy were verified by including blind replicate samples in each batch (n = 4) and were routinely checked using reference and blank materials. All quality control measures confirmed that the analytical results for both MPs and TPH were reliable and reproducible.

3. Results and discussion

3.1. Abundance and morphological characteristics of MPs

MP concentrations exhibited pronounced spatial variability across the sampling stations in both water and sediment environments (Table S1). In water samples, concentrations ranged from 0.05 MPs L^{-1} at Station S3 (the least contaminated site) to 2.3 MPs L^{-1} at Station S5, which appeared to be influenced by nearby human activities and hydrodynamic retention. Additional localized hotspots were observed at S8, S9, and S13 (≈1.0–1.35 MPs L^{-1}), suggesting enhanced MP input from domestic effluent pathways or shoreline usage. In contrast, relatively low concentrations at S4, S10, and S14 (<0.6 MPs L^{-1}) indicate reduced anthropogenic pressure or stronger flushing and dispersion processes. Sediment concentrations also varied markedly among stations, ranging from 2.01 MPs kg^{-1} at S9, where higher hydrodynamic energy may prevent fine particle retention, to 24.13 MPs kg^{-1} at S14, the most impacted area with enhanced depositional conditions. Elevated sediment loads at S12 (16 MPs kg^{-1}) and S13 (23.06 MPs kg^{-1}) further demonstrate that calmer hydrodynamic regimes and proximity to land-based sources facilitate MP accumulation. Intermediate levels at stations such as S2, S3, S7, and S8 (9–12 MPs kg^{-1}) reflect moderate retention conditions, while S1, S4, and S5 (6–8 MPs kg^{-1}) exhibited modest but consistent microplastic deposition. These site-specific differences underscore the strong influence of local hydrodynamics, sedimentation patterns, and proximity to pollution sources on MP distribution across the study area. When compared with previous studies, the concentrations observed in this research fall within the moderate range of coastal environments. Sánchez-Campos et al. (2024) reported significantly higher concentrations in a Mexican coastal lagoon (7.5 ± 5.3 MPs L^{-1}), indicating that anthropogenic pressure and watershed characteristics differ markedly from those of our study region [28]. Sediment concentrations in the present study were also substantially lower than those reported by Firdaus et al. (2020), who documented abundances up to 590 MPs kg^{-1} in Indonesian coastal sediments nearly an order of magnitude greater than the highest concentrations measured at our sites [29]. Such disparities highlight that plastic input intensity, geomorphology, and retention capacity vary substantially across global coastal systems. Across all stations, MP particle sizes ranged from <100 µm to >3000 µm, with the 100–500 µm and 500–1000 µm fractions consistently dominating in both water and sediment (Fig. 3A). The predominance of the 100–500 µm class—which represented the largest proportion of particles at nearly all stations suggests that secondary MPs derived from fragmentation processes constitute the major component of contamination. This pattern is consistent with findings from the Bohai Sea [30] and coastal regions of the Persian Gulf [31]. Environmental processes, such as fragmentation and weathering, likely influence the prevalence of smaller MP particles. In terms of morphology, fibers and films were the dominant particle types across stations, while fragments occurred less frequently (Fig. 3B). Fiber dominance in stations with higher water column concentrations (e.g., S5, S8, S13) may be linked to the transport of textile-derived fibers in domestic wastewater. This observation aligns with Claessens et al. (2011), who identified fibers as the most abundant MP type in Belgian coastal sediments [32]. The higher proportion of films in depositional stations such as S12–S14 suggests that degraded packaging materials and film-like plastics preferentially settle, an observation consistent with hydrodynamic expectations. Fiber persistence in the water column likely reflects their elongated geometry and low settling velocity [9]. Color analysis revealed that black, red, and brown MPs dominated both matrices across nearly all sites, followed by blue and orange particles (Fig. 3C). Sites with greater anthropogenic influence (e.g., S5, S8, S13) exhibited higher proportions of dark-colored MPs, which are often associated with aged plastics, tire wear, and fishing gear. In contrast, stations with heavy

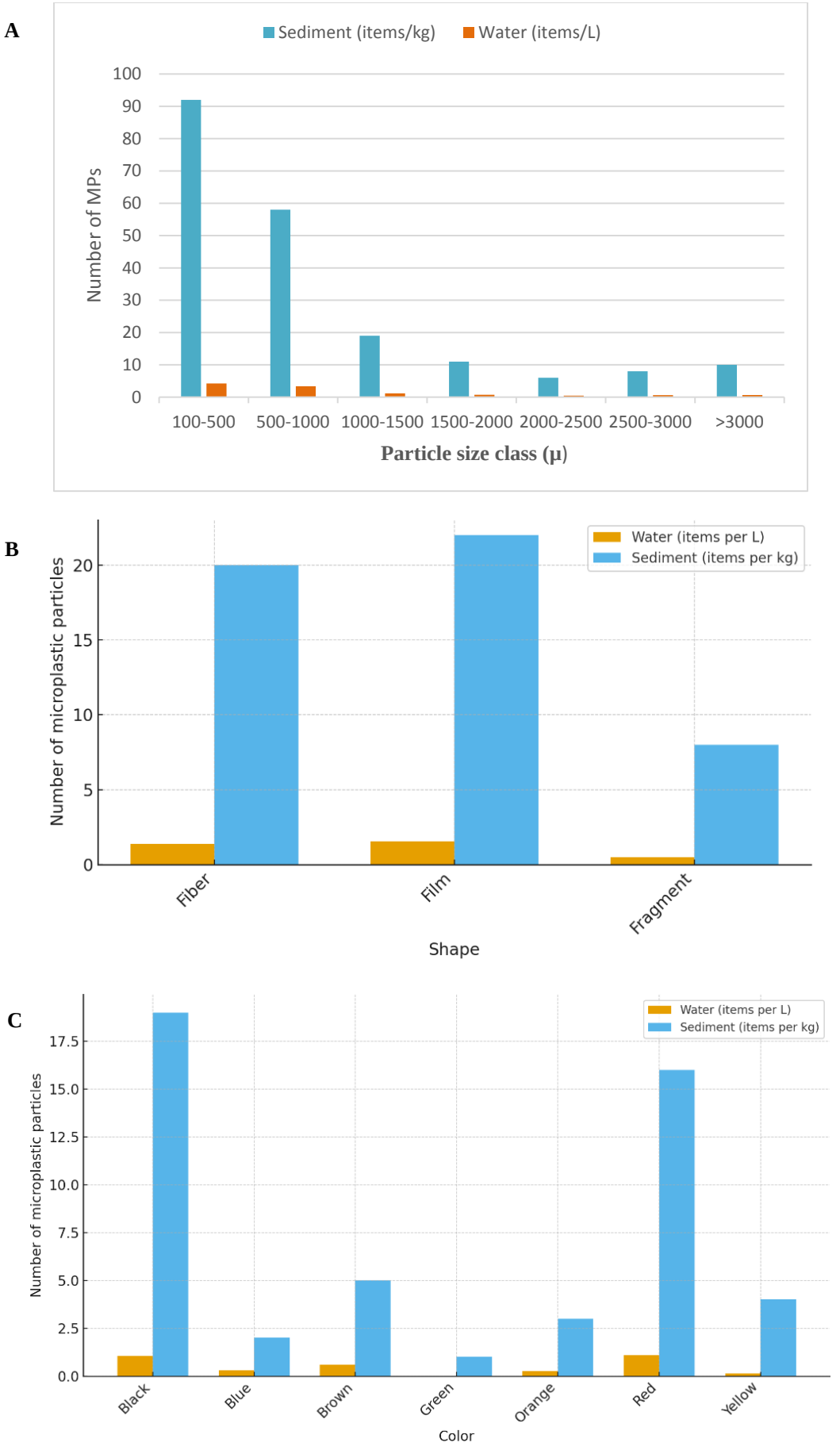

Figure 3. Size, shape, and color distribution of microplastics in water and sediment samples

sediment accumulation (S12–S14) contained more faded or photodegraded particles, consistent with long-term environmental exposure. Photobleaching processes described by Kalogerakis et al. (2017) and color loss documented by Li et al. (2024) support this interpretation.

3.2. Chemical identification of MPs

Raman spectroscopy was used to identify the chemical composition of MP particles in both water and sediment samples. Based on the obtained spectra, several polymer types were detected, including polyethylene (PE), polyethylene–acrylic acid (PEAA), polyvinyl (PV), polystyrene (PS), and polyethylene terephthalate (PET) (Fig. S1). Among these, PE and PET showed the highest frequency of occurrence in both water and sediment samples (Fig. 4). The dominance of these two polymers reflects their widespread use in packaging materials, single-use products, and synthetic textiles, which are considered major sources of MP contamination in coastal environments.The polymer composition observed in this study is consistent with previous findings reported from various locations along the Persian Gulf and the Oman Sea, where PE, PET, PS, and nylon were identified as the most common polymers in marine sediments and surface waters. A similar pattern has also been documented globally, as these polymers are characterized by low density, high buoyancy, and extensive use in consumer products, which facilitate their transport and accumulation in aquatic systems [33-35].

3.3. TPH concentrations in sediment and water

The concentrations of total petroleum hydrocarbons (TPHs) showed pronounced site-specific variability across the fourteen sampling stations (Tables S2–S5). In sediments, TPH values ranged from 8.37 µg/kg at S7 to 1835.29 µg/kg at S8, indicating more than a 200-fold difference among sites. Stations S8, S13, S6, S11, and S3 exhibited the highest sedimentary TPH levels (1835.29, 1241.94, 1184.10, 984.83, and 810.32 µg/kg, respectively), while S7, S5, and S9 showed the lowest concentrations (8.37, 45.24, and 115.97 µg/kg). The elevated concentrations at S8 and S13 are likely influenced by the proximity of riverine inputs and localized anthropogenic pressures. In water samples, TPH concentrations ranged from non-detectable levels at S2, S3, and S13 to a maximum of 20.15 µg/L at S11. Elevated concentrations were also observed at S12 (19.03 µg/L), S7 (12.72 µg/L), and S14 (10.40 µg/L), whereas lower levels (<1 µg/L) were recorded at S1, S8, S9, and S10. The distinctly high TPH concentration at S11—nearly twice that of most other stations—suggests the presence of strong local contamination sources, most likely related to maritime traffic, small-scale harbor activities, or discharges from nearby urban areas, similar to trends reported by Escher et al. (2011). In general, sediment samples exhibited substantially higher TPH concentrations than water samples. This pattern reflects the strong hydrophobicity, chemical stability, and particle affinity of petroleum hydrocarbons, which promote their accumulation and persistence in sediments [36, 37]. Consistent with findings from other coastal regions, such as the northern Persian Gulf, spatial heterogeneity in hydrocarbon contamination is commonly associated with harbors, industrial zones, and areas impacted by petroleum-related activities [31, 36]. The sediment-bound hydrocarbons may act as long-term reservoirs of contamination, posing potential ecological risks to benthic organisms. The strong affinity of TPH compounds for sediment particles facilitates their accumulation, while their low water solubility limits their concentration in the overlying water column [38]. However, the presence of measurable concentrations in both water and sediment indicates ongoing inputs and persistence of petroleum hydrocarbons in the studied area.

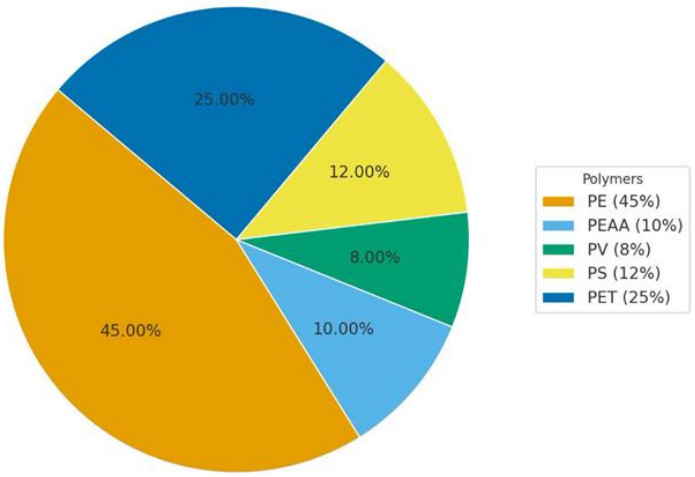

Figure 4. Polymer composition of microplastics in water and sediment samples

This situation may contribute to chronic exposure for marine organisms and potentially lead to bioaccumulation in the food web.

3.4. Spatial pattern of TPH and MPs

The spatial pattern of TPH and MPs in water and sediments revealed clear variability among stations with no spatial overlap between the highest concentrations of the two pollutants. The maximum number of MPs in water was recorded at station 5, while in sediments it occurred at station 14 (Table S1). In contrast, the highest TPH concentrations were observed at station 11 in water and station 8 in sediments (Tables S2 and S3). This lack of overlap suggests that TPH and MPs behave differently in the environment. Petroleum hydrocarbons tend to accumulate in sediments due to their hydrophobic and persistent nature, whereas MPs may disperse more heterogeneously depending on size, density, polymer type, and hydrodynamic conditions. Unlike hydrocarbons, MPs are more mobile and influenced by currents and wind-driven transport, leading to irregular distribution patterns. Similar mismatches in spatial distribution between different pollutants have been reported in other coastal ecosystems [27, 31]. Similarly, while TPH is often associated with point sources such as shipping and industrial discharges, MPs generally originate from diffuse sources such as urban runoff, fishing activities, and the breakdown of larger debris.

4. Conclusion

The clear divergence in spatial distribution between MPs and petroleum hydrocarbons in the Caspian Sea's coastal waters reveals their distinct environmental pathways. This separation underscores how these pollutants originate from different sources and behave independently in the marine environment. While fragmented plastic debris from urban waste dominates the microplastic profile, petroleum hydrocarbons show concentrated patterns near industrial and shipping activities. As a semi-enclosed basin with limited water exchange, the Caspian Sea demonstrates particular vulnerability to accumulating both particulate and chemical pollutants. The simultaneous presence of these contaminants, even in different spatial patterns, suggests potential compounded ecological effects - especially concerning if MPs act as carriers for hydrophobic petroleum compounds. Consequently, safeguarding the Caspian Sea ecosystem necessitates a strategic shift towards integrated monitoring and source-specific mitigation to effectively manage its complex contaminant profile. Future research should focus on understanding the interaction mechanisms between these pollutants and their biological impacts on marine organisms.

Acknowledgements

This research is extracted from the dissertation of the PhD student in Environmental Engineering, Islamic Azad University of Ardabil Branch with the dissertation code of 162853135. Therefore, the authors appreciate the esteemed president, educational and research deputies of Ardabil Islamic Azad University for their cooperation in facilitating the implementation of this project.

Funding

The research project has been reviewed and granted funding by the Islamic Azad University of Ardabil Branch.

Authors Contribution
R.SH: collected and analyzed samples. **E.F:** Project administration, Supervisor, Visualization, Writing – review & editing. **A.M:** Visualization, Laboratory Analysis. **M.HN:** Project administration, Visualization, Writing – Original Draft, Writing – review & editing. **H.S**: Visualization, Locating the sampling site.

Availability of data and materials
All relevant data are included in the paper or its supplementary information.

Conflict of interests
The authors declare that they have no known competing financial interests or personal relationships that could have appeared to influence the work reported in this paper.

References

[1] Niari, M.H., Takdastan, A., Babaei, A., Dobaradaran, S., Jorfi, S. and Ahmadi, M. (2024). Fate and ecological risk of phthalate esters in microplastics of wastewater in the wastewater treatment plant. *Water, Air, & Soil Pollution*, 235, pp. 106.

[2] Thanigaivel, S., Kamalesh, R., Ragini, Y., Saravanan, A., Vickram, A., Abirami, M. and Thiruvengadam, S. (2025). Microplastic pollution in marine environments: An in-depth analysis of advanced monitoring techniques, removal technologies, and future challenges. *Marine Environmental Research*, pp. 106993.

[3] Niari, M.H., Ghobadi, H. and Aslani, M.R. (2025). Quantification of microplastics and phthalate esters in nasal lavage fluid of hospital employees after face mask use. *Water, Air, & Soil Pollution*, 236, pp. 130.

[4] Cole, M., Lindeque, P., Halsband, C. and Galloway, T.S. (2011). Microplastics as contaminants in the marine environment: a review. *Marine Pollution Bulletin*, 62, pp. 2588–2597.

[5] Nematollahi, M.J., Moore, F., Keshavarzi, B., Vogt, R.D., Saravi, H.N. and Busquets, R. (2020). Microplastic particles in sediments and waters, south of Caspian Sea: Frequency, distribution,

characteristics, and chemical composition. *Ecotoxicology and Environmental Safety*, 206, pp. 111137.

[6] Manbohi, A., Mehdinia, A., Rahnama, R. and Dehbandi, R. (2021). Microplastic pollution in inshore and offshore surface waters of the southern Caspian Sea. *Chemosphere*, 281, pp. 130896.

[7] Wright, S.L., Thompson, R.C. and Galloway, T.S. (2013). The physical impacts of microplastics on marine organisms: a review. *Environmental Pollution*, 178, pp. 483–492.

[8] Nawaz, F., Islam, Z.U., Ghori, S.A., Bahadur, A., Ullah, H., Ahmad, M. and Khan, G.u. (2025). Microplastic and nanoplastic pollution: Assessing translocation, impact, and mitigation strategies in marine ecosystems. *Water Environment Research*, 97, pp. e70032.

[9] Foshtomi, M.Y., Oryan, S., Taheri, M., Bastami, K.D. and Zahed, M.A. (2019). Composition and abundance of microplastics in surface sediments and their interaction with sedimentary heavy metals, PAHs and TPH (total petroleum hydrocarbons). *Marine Pollution Bulletin*, 149, pp. 110655.

[10] Bakir, A., Rowland, S.J. and Thompson, R.C. (2014). Enhanced desorption of persistent organic pollutants from microplastics under simulated physiological conditions. *Environmental Pollution*, 185, pp. 16–23.

[11] Chen, C.-L. (2015). Regulation and management of marine litter. *In Marine Anthropogenic Litter, Springer International Publishing, Cham*, pp. 395–428.

[12] Zhong, L., Wang, R., Wang, P., Yu, G., Song, Y. and Sun, F. (2025). Enhanced remediation of petroleum in soil by petroleum-degrading bacterium strain TDYN1 and the effects of microplastics. *Bulletin of Environmental Contamination and Toxicology*, 114, pp. 81.

[13] Emadi Jamali, M., Mousavi Nadushan, R., Javid, A.H., Mashinchiyan Moradi, A. and Givianrad, M.H. (2020). Spatial trends of Total Petroleum Hydrocarbons, related heavy metals and sediment characteristics in South Caspian Sea: Effect of depth and temporal dispersions. *Iranian Journal of Fisheries Sciences*, 19, pp. 3221–3238.

[14] Lundgreen, K., Holbech, H., Pedersen, K.L., Petersen, G.I., Andreasen, R.R., George, C., Drillet, G. and Andersen, M. (2018). UV fluences required for compliance with ballast water discharge standards using two approved methods for algal viability assessment. *Marine Pollution Bulletin*, 135, pp. 1090–1100.

[15] Gholizadeh, M. and Cera, A. (2022). Microplastic contamination in the sediments of Qarasu estuary in Gorgan Bay, south-east of Caspian Sea, Iran. *Science of the Total Environment*, 838, pp. 155913.

[16] Manbohi, A., Mehdinia, A., Rahnama, R., Hamzehpour, A. and Dehbandi, R. (2023). Sources and hotspots of microplastics of the rivers ending to the southern Caspian Sea. *Marine Pollution Bulletin*, 188, pp. 114562.

[17] Gholizadeh, M., Bagheri, T., Harsij, M., Danabas, D., Zakeri, M.A.M. and Siddique, M.A.M. (2024). Assessment of microplastic contamination in some commercial fishes of the southern Caspian Sea and its potential risks. *Environmental Science and Pollution Research*, 31, pp. 26006–26018.

[18] Razeghi, N., Hamidian, A.H., Wu, C., Zhang, Y. and Yang, M. (2021). Microplastic sampling techniques in freshwaters and sediments: a review. *Environmental Chemistry Letters*, 19, pp. 4225–4252.

[19] Stock, F., Kochleus, C., Bänsch-Baltruschat, B., Brennholt, N. and Reifferscheid, G. (2019). Sampling techniques and preparation methods for microplastic analyses in the aquatic environment–A review. *TrAC Trends in Analytical Chemistry*, 113, pp. 84–92.

[20] Niari, M.H., Ghobadi, H., Amani, M., Aslani, M.R., Fazlzadeh, M., Matin, S., Takaldani, A.H.S. and Hosseininia, S. (2025). Characteristics and assessment of exposure to microplastics through inhalation in indoor air of hospitals. *Air Quality, Atmosphere & Health*, 18, pp. 253–262.

[21] Elkhatib, D. and Oyanedel-Craver, V. (2020). A critical review of extraction and identification methods of microplastics in wastewater and drinking water. *Environmental Science & Technology*, 54, pp. 7037–7049.

[22] Takdastan, A., Niari, M.H., Babaei, A., Dobaradaran, S., Jorfi, S. and Ahmadi, M. (2021). Occurrence and distribution of microplastic particles and the concentration of Di 2-ethyl hexyl phthalate (DEHP) in microplastics and wastewater in the wastewater treatment plant. *Journal of Environmental Management*, 280, pp. 111851.

[23] Balasubramaniam, D.A., Panneerselvam, R., Akshaya, K., Rajamanickam, R., De-la-Torre, G.E. and Selvasembian, R. (2024). The advancements and detection methodologies for microplastic detection in environmental samples. *In Microplastics: Environmental Pollution and Degradation Process, Springer*, pp. 207–224.

[24] Chen, H., Jiang, F., Li, J., Cao, W., Zhang, D., Zhang, F., Wang, S. and Sun, C. (2025). Interlinked water and sediment microplastics in the Laizhou Bay of China. *Journal of Oceanology and Limnology*, 43, pp. 446–458.

[25] Niari, M.H., Jaafarzadeh, N., Dobaradaran, S., Niri, M.V. and Dargahi, A. (2023). Release of microplastics to the environment through wastewater treatment plants: Study on four types of wastewater treatment processes. *Water, Air, & Soil Pollution*, 234, pp. 589.

[26] Samaei, S.H.-A., Mojahednia, P., Chen, J., Li, Z., Jaszczyszyn, K., Kiedrzyńska, E. and Xue, J. (2025). What Does the "Trojan Horse" Carry? The Pollutants Associated with Microplastics/Nanoplastics in Water Environments. *ACS ES&T Water*, 5, pp. 1530–1545.

[27] Abdykarimov, B., Alimzhanova, M., López-Serna, R. and Syrgabek, Y. (2025). Green Analytical Procedure Index Assessment for Total Petroleum Hydrocarbons Determination Methods in Soil and Sediments. A Review. *Trends in Environmental Analytical Chemistry*, pp. e00262.

[28] Sánchez-Campos, M., Ponce-Vélez, G., Sanvicente-Añorve, L. and Alatorre-Mendieta, M. (2024). Microplastic contamination in three environmental compartments of a coastal lagoon in the southern Gulf of Mexico. *Environmental Monitoring and Assessment*, 196, pp. 1012.

[29] Firdaus, M., Trihadiningrum, Y. and Lestari, P. (2020). Microplastic pollution in the sediment of Jagir estuary, Surabaya City, Indonesia. *Marine Pollution Bulletin*, 150, pp. 110790.

[30] Zhang, M., Lin, Y., Booth, A.M., Song, X., Cui, Y., Xia, B., Gu, Z., Li, Y., Liu, F. and Cai, M. (2022). Fate, source and mass budget of sedimentary microplastics in the Bohai Sea and the Yellow Sea. *Environmental Pollution*, 294, pp. 118640.

[31] Naji, A., Nuri, M. and Vethaak, A.D. (2018). Microplastics contamination in molluscs from the northern part of the Persian Gulf. *Environmental Pollution*, 235, pp. 113–120.

[32] Claessens, M., De Meester, S., Van Landuyt, L., De Clerck, K. and Janssen, C.R. (2011). Occurrence and distribution of microplastics in marine sediments along the Belgian coast. *Marine Pollution Bulletin*, 62, pp. 2199–2204.

[33] Fan, S., Yan, Z., Qiao, L., Gui, F., Li, T., Yang, Q., Zhang, X. and Ren, C. (2023). Biological effects on the migration and transformation of microplastics in the marine environment. *Marine Environmental Research*, 185, pp. 105875.

[34] Saeed, T., Al-Jandal, N., Al-Mutairi, A. and Taqi, H. (2020). Microplastics in Kuwait marine environment: Results of first survey. *Marine Pollution Bulletin*, 152, pp. 110880.

[35] Karkanorachaki, K., Syranidou, E. and Kalogerakis, N. (2021). Sinking characteristics of microplastics in the marine environment. *Science of the Total Environment*, 793, pp. 148526.

[36] Quilliam, R.S., Jamieson, J. and Oliver, D.M. (2014). Seaweeds and plastic debris can influence the survival of faecal indicator organisms in beach environments. *Marine Pollution Bulletin*, 84, pp. 201–207.

[37] Chapman, P.M. (2017). Assessing and managing stressors in a changing marine environment. *Marine Pollution Bulletin*, 124, pp. 587–590.

[38] Adeniji, A.O., Okoh, O.O. and Okoh, A.I. (2017). Petroleum hydrocarbon profiles of water and sediment of Algoa Bay, Eastern Cape, South Africa. *International Journal of Environmental Research and Public Health*, 14, pp. 1263.